WHO IS MORE AT RISK IN HETEROGENOUS NETWORKS?

June Zhang

University of Hawai'i at Mānoa
Electrical Engineering
Honolulu, HI, 96822

José M.F. Moura

Carnegie Mellon University
Electrical and Computer Engineering
Pittsburgh, PA, 15213

ABSTRACT

Network-based epidemics models try to characterize the impact of network topology, which represents contagion pathways, on the spread of infection. Although these models explicitly consider the dynamics of individuals in the given network (i.e., the state of the system is $\mathbf{x}(t) = [x_1(t), x_2(t), \ldots, x_N(t)]^T$), analysis has focused on characterizing the vulnerability of the *entire* population rather than the vulnerability of the individuals in the population. We focus on characterizing the vulnerability of the ith individual in the network by studying the marginal probability of infection, $P(x_i = 1)$, of the scaled SIS process. Studying the vulnerability of individuals is important because it may be tempting to assume that $P(x_i = 1)$ is related to the degree of the ith node. Since infection rate is usually assumed to be dependent on the number of infected neighbors, then it seems reasonable that nodes with more connections (i.e., higher degree) would be more at risk. We show that this is *not* always true. Further, with a closed-form approximation of $P(x_i = 1)$, as solving for the exact probability requires the summation of 2^N terms, we characterize the conditions for when degree distribution is a good indicator of how susceptible an individual is to infection.

Index Terms— network science, scaled SIS process, network process, marginal probability, Markov network

1. INTRODUCTION

Classic compartmental epidemics models study the dynamics of the total number (or percentage) of infected and/or healthy individuals in a population. In contrast, network-based epidemics models characterize the dynamics of N-individuals in a network (i.e., $\mathbf{x}(t) = [x_1(t), x_2(t), \ldots, x_N(t)]^T$) while explicitly accounting for some network structure describing significant contacts (i.e., potential contagion pathways) between individuals [1, 2, 3, 4, 5, 6]; in these models, the infection rate of a susceptible is assumed to depend on its number of infected neighbors, thereby coupling the network structure to the dynamics of the epidemics.

One question of interest is the impact of network structure on the epidemics dynamics. However, network-based epidemics model, despite characterizing the dynamics of $\mathbf{x}(t)$, has primarily focused on analyzing the same *macroscopic* quantities, such as the percentage of infected individuals, as classic epidemics models. Reference [7] showed a relationship between the spectral radius of the adjacency matrix and the epidemics threshold.

In this paper, we focus instead on analyzing the *microscopic* vulnerability of each of the N individuals in the population and and its relationship to the network structure. Adopting the scaled susceptible-infected-susceptible (SIS) process introduced in [8, 9], we study microscopic vulnerability using $P(x_i = 1)$, the probability of infection of the ith agent. In particular, we are interested in how $P(x_i = 1)$ depends on the underlying network structure. Since in network-based epidemics models, the infection rate of an individual is dependent on its number of infected neighbors, it is reasonable to assume that individuals with *higher* degree are *more* vulnerable to infection. We show by analyzing a closed-form approximation of $P(x_i = 1)$ that this is *not* necessarily correct —the coupling between network structure and dynamics parameters results in a more subtle relationship between network structure and $P(x_i = 1)$.

Section 2 reviews network-based epidemics models, specifically details the dynamics of the scaled SIS process. Section 3 shows with a simple example that the marginal probability of infection, $P(x_i = 1)$, demonstrates 3 types of behaviors: 1) $P(x_i = 1)$ is approximately the same for all the nodes; 2) $P(x_i = 1)$ can be ordered by nodal degree; and 3) $P(x_i = 1)$ is not approximately the same for all the nodes nor can it necessarily be ordered by nodal degree. While the exact computation of $P(x_i = 1)$ is infeasible since it involves knowing the partition function, which requires a summation of 2^N terms, section 4 presents a closed-form approximation of $P(x_i = 1)$ that holds for certain dynamics and also explains the 3 observed types of behavior. Section 5 concludes the paper.

2. BACKGROUND: SCALED SIS PROCESS

Network-based epidemics models explicitly account for an arbitrary, heterogeneous network, $G(V, E)$, whose edges represent potential infection transmission pathways. Typically, the network is assumed to remain static in time. We also assume that it is unweighted and undirected. Similar to other stochastic network-based epidemics models such as the contact process [10, 11, 12], the scaled SIS process, introduced in [8], is a (continuous-time) Markov process. At any time $t \geq 0$, the state of the population is described by the configuration

$$\mathbf{x}(t) = [x_1(t), x_2(t), \ldots, x_N(t)]^T,$$

where $x_i(t)$ is the state of the ith individual at time t. We assume that an individual can either be healthy ($x_i(t) = 0$) or infected ($x_i(t) = 1$).

Let $T_i^+\mathbf{x}$ denote the configuration that is the same as $\mathbf{x}$ except that the ith individual becomes infected, and let $T_j^-\mathbf{x}$ denote the configuration that is the same as $\mathbf{x}$ except that the jth individual heals. The scaled SIS process assumes that

1. $X(t)$ transitions to a configuration where the jth agent, $j = 1, \ldots, N$, is healed with transition rate:

$$q(\mathbf{x}, T_j^-\mathbf{x}) = \mu, \quad \mathbf{x} \neq T_j^-\mathbf{x}. \tag{1}$$

This work was partially supported by NSF grants CCF1011903 and CCF1513936

2. $X(t)$ transitions to a configuration where the ith agent, $i = 1, 2, \ldots, N$, is infected with transition rate

$$q(\mathbf{x}, T_i^+\mathbf{x}) = \lambda\gamma^{m_i}, \quad \mathbf{x} \neq T_i^+\mathbf{x}. \tag{2}$$

where $m_i = \sum_{j=1}^{N} \mathbf{A}_{ij}x_j$ is the number of infected neighbors of node i. The matrix $\mathbf{A} = [\mathbf{A}_{ij}]$ is the adjacency matrix of $G(V, E)$.

The parameter $\mu > 0$ is the healing rate. The parameter $\lambda > 0$ is the exogenous (i.e., spontaneous) infection rate—when $m_i = 0$, the infection rate is λ. The parameter $\gamma > 0$ is the endogenous (i.e., contagion) infection factor; it is unit-less and accounts for the number of infected neighbors. The state space of the scaled SIS process is $\mathcal{X} = \{\mathbf{x}\}$ and the size of the state space is 2^N.

There are three major differences between the scaled SIS process and other common stochastic network-based models: 1) we assume that infection can come from outside the population. This means that there is no absorbing Markov state since a healthy individual always has a nonzero probability of becoming infected; 2) the infection rate depends exponentially on the number of neighbors instead of linearly. We discussed the difference between linear dependence versus exponential dependence in [13]; 3) lastly, the scaled SIS process has a closed-form equilibrium distribution, $\pi(\mathbf{x})$, that describes the behavior of the process for $t \to \infty$ (we drop the dependence of the network configuration $\mathbf{x}$ on time to denote that the process has reached equilibrium):

$$\pi(\mathbf{x}) = \frac{1}{Z}e^{H(\mathbf{x})}, \quad \mathbf{x} \in \mathcal{X} \tag{3}$$

where Z is the partition function and is defined as

$$Z = \sum_{\mathbf{x}\in\mathcal{X}} \left(\frac{\lambda}{\mu}\right)^{1^T\mathbf{x}} \gamma^{\frac{\mathbf{x}^T\mathbf{A}\mathbf{x}}{2}}. \tag{4}$$

The negative of $H(\mathbf{x})$, $-H(\mathbf{x})$, is the Hamiltonian and represents the energy of a configuration $\mathbf{x}$. The exponent $H(\mathbf{x})$ is

$$H(\mathbf{x}) = 1^T\mathbf{x}\log\left(\frac{\lambda}{\mu}\right) + \frac{\mathbf{x}^T\mathbf{A}\mathbf{x}}{2}\log(\gamma). \tag{5}$$

3. INDIVIDUAL VULNERABILITY TO INFECTION

In this paper, we focus on studying the vulnerability of individual agents to infection rather than the susceptibility of the entire population. The vulnerability of the ith individual can be characterized by how likely it is to be infected at some time $t \geq 0$, $P(x_i(t) = 1) \in [0, 1]$. We are particularly interested in understanding how $P(x_i(t) = 1)$ depends on the networks structure; it is important then to study the marginal probabilities at equilibrium since $P(x_i(0) = 1) = 1$ for any infection source; the transient behavior of marginal probabilities depends more on the location of the infection source, which may be independent of the network topology.

At equilibrium, the marginal (i.e., singleton) probability of infection of the scaled SIS process is :

$$\lim_{t\to\infty} P(x_i(t) = 1) = P(x_i = 1) = \sum_{\mathbf{x}\in\mathcal{X}:x_i=1} \pi(\mathbf{x}) = \frac{1}{Z}\sum_{\mathbf{x}\in\mathcal{X}:x_i=1} e^{H(\mathbf{x})}, \tag{6}$$

where $\pi(\mathbf{x})$ is the equilibrium distribution (3) and $H(\mathbf{x})$ is defined in (5).

For small networks (i.e., $N \leq 20$ means $|\mathcal{X}| \leq 2^{20}$), we can compute $P(x_i = 1)$ exactly at all nodes. Figure 2 shows $P(x_i = 1)$ for selected nodes of a 16-node network (see Figure 1a). As $P(x_i = 1)$ also depends on the dynamics parameters $\frac{\lambda}{\mu}$ and γ, we set $\frac{\lambda}{\mu}$ to a constant value and change γ to study the behavior of $P(x_i = 1)$; as γ increases, the infection rate due to contagion increases, and we expect that $P(x_i = 1)$ will increase to 1 for all the nodes. In particular, we consider $P(x_i = 1)$ for 5 different nodes: $i = 1, 5, 6, 9, 10$. In the underlying network, node 1 has 5 neighbors node 5 has 2 neighbors, node 6 has 3 neighbors, node 9 has 4 neighbors and node 10 has 2 neighbors.

In Figure 2a ($\frac{\lambda}{\mu} = 0.6895$ and $\gamma \in [1, 10]$), $P(x_1 = 1) \geq P(x_9 = 1) \geq P(x_6 = 1) \geq P(x_5 = 1) \geq P(x_{10} = 1)$; the marginal probability of infection can be ordered by the degree of the node in the underlying network. However, in Figure 2b ($\frac{\lambda}{\mu} = 0.00025, \gamma \in [1, 1200]$), with a different range of dynamics parameters, $P(x_1 = 1) \geq P(x_5 = 1) \geq P(x_{10} = 1) \geq P(x_9 = 1) \geq P(x_6 = 1)$; in this case, the marginal probability of infection *can not* be ordered by the nodal degree.

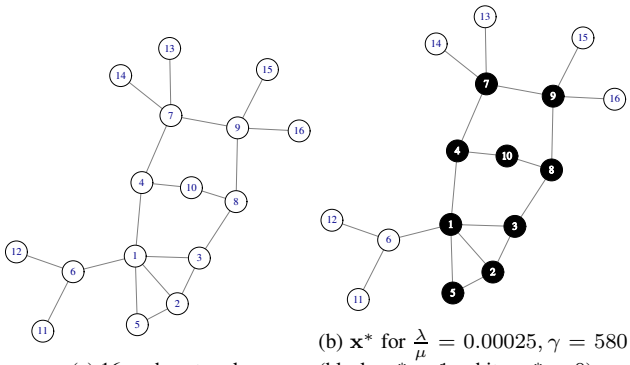

(a) 16-node network

(b) $\mathbf{x}^*$ for $\frac{\lambda}{\mu} = 0.00025, \gamma = 580$ (black: $x_i^* = 1$, white: $x_i^* = 0$)

Fig. 1: 16-node network

From this simple example, we see there are roughly three types of behaviors that characterize the marginal probability at equilibrium:

Type 1: $P(x_i = 1) \approx P(x_j = 1), \forall i, j = 1, 2, \ldots, N, i \neq j$

Type 2: Let k_i denote the degree of the ith node in the underlying network $G(V, E)$. If $k_i > k_j$, then $P(x_i = 1) > P(x_j = 1)$

Type 3: Let k_i denote the degree of the ith node in the underlying network $G(V, E)$. If $k_i > k_j$, it is possible that $P(x_i = 1) < P(x_j = 1)$

For type 1), the network structure does not affect the marginal probabilities since all nodes have similar probability of being infected; for type 2), only the local description of the network matters since the marginal probabilities of infection can be ranked by the node degree in the underlying network $G(V, E)$; and for type 3), the local description of the network is not sufficient to rank the marginal probabilities since the $P(x_i = 1)$ may not necessarily be ordered by the nodal degree.

When the network is large, exact computation of marginal probabilities (6) becomes prohibitively expensive; these probabilities may be approximated by sampling method [14]. In the next section, we approximate by a closed-form expression the marginal probabilities $\widehat{P}(x_i = 1)$; this approximation gives insight into the three types of observed behavior.

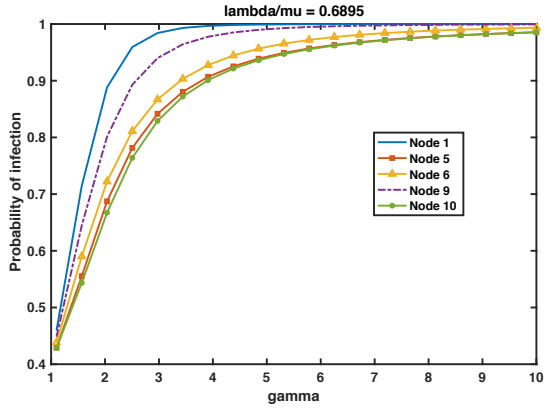

(a) $P(x_i = 1)$ for $\frac{\lambda}{\mu} = 0.6895, \gamma \in [1, 10]$

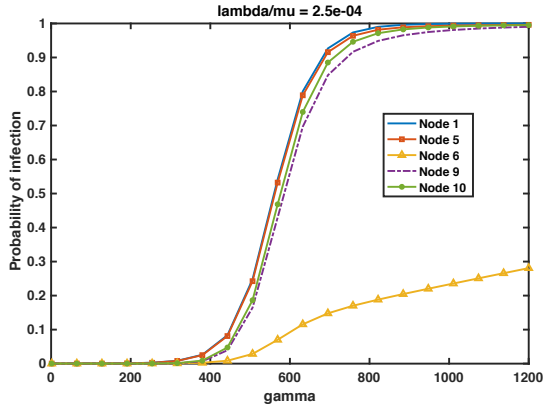

(b) $P(x_i = 1)$ for $\frac{\lambda}{\mu} = 0.00025, \gamma \in [1, 1200]$

Fig. 2: $P(x_1 = 1), P(x_5 = 1), P(x_6 = 1), P(x_9 = 1), P(x_{10} = 1)$ for Different Dynamics Parameters

4. APPROXIMATING MARGINAL PROBABILITIES

We find a reasonable approximation to the marginal probability of infection, $\widehat{P}(x_i = 1) \approx P(x_i = 1)$, for all nodes in an underlying network.

Theorem 4.1. *[Proof in Appendix] Consider a scaled SIS process with parameters λ, μ, γ with underlying network structure $G(V, E)$ and most-probable configuration $\mathbf{x}^* = [x_1^*, x_2^*, \ldots, x_N^*]^T$, where*

$$\mathbf{x}^* = \arg\max_{\mathbf{x} \in \mathcal{X}} \quad \pi(\mathbf{x}).$$

If $e^{H(\mathbf{x}^*)} >> e^{H(\mathbf{x})}, \forall \mathbf{x} \in \mathcal{X} \setminus \mathbf{x}^*$, where $H(\cdot)$ is the exponent of the equilibrium distribution (5) *and*

$$m_i^* = \sum_{j=1}^{N} \mathbf{A}_{ij} x_j^*,$$

then

$$P(x_i = 1) \approx \widehat{P}(x_i = 1) = \frac{1}{1 + \left(\frac{\lambda}{\mu}\gamma^{m_i^*}\right)^{-1}} \tag{7}$$

In general, the marginal probabilities of infection (6) can not be described in closed-form. However, with the condition that $e^{H(\mathbf{x}^*)} >> e^{H(\mathbf{x})}, \forall \mathbf{x} \in \mathcal{X} \setminus \mathbf{x}^*$, meaning that the probability of the most-probable configuration significantly dominates over the other $2^N - 1$ configurations in the equilibrium distribution, then Theorem 4.1 tells us that $P(x_i = 1)$ can be approximated in closed-form by (7). Figure 3 shows the normalized ℓ_2 difference between the true $P(x_i = 1)$ and the approximate $\widehat{P}(x_i = 1)$ for the 16-node network shown in Figure 1a with different $\frac{\lambda}{\mu}$ and γ values. The maximum deviation between the approximation to the true value is 1. We see that the closed-approximation (7) is good for some ranges of dynamics parameters but poor for others; this depends on when the condition of Theorem 4.1 is satisfied or not.

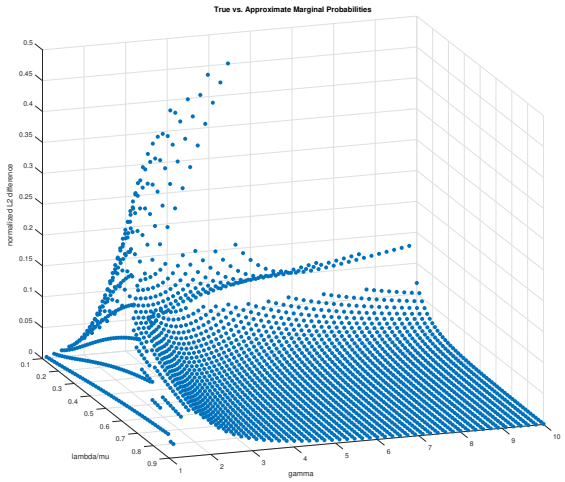

Fig. 3: ℓ_2 error: $\sqrt{\frac{1}{N}\sum_{i=1}^{N}(P(x_i = 1) - \widehat{P}(x_i = 1))^2}$

While the closed-form approximation is not universally good for all parameter values, it gives insight on understanding the three behavior types since $\widehat{P}(x_i = 1)$ depends only on the most-probable configuration $\mathbf{x}^*$ rather than having to marginalize over 2^{N-1} configurations. When $\mathbf{x}^* = \mathbf{x}^0 = [0, 0, \ldots, 0]$, then m_i^* is the same for every node (i.e., zero), Therefore, we expect $\widehat{P}(x_i = 1)$ to be the same for all the nodes. This results in type 1 behavior. We see this in both Figure 2a and Figure 2b when the endogenous infection factor γ is small.

When $\mathbf{x}^* = \mathbf{x}^N = [1, 1, \ldots, 1]$, then m_i^* is equal to the degree of the ith node in the underlying network. Assuming that $\gamma > 1$, then nodes with larger number of neighbors in $G(V, E)$ will have higher probability of being infected. This results in type 2 behavior. This is the behavior we see in Figure 2a. However, with high enough infection rates λ and/or γ, then $\widehat{P}(x_i = 1)$ saturates to 1 for all the nodes, resulting again in type 1 behavior.

Type 3 behavior, which we see in Figure 2b is the most interesting. We showed in [9] that $\mathbf{x}^*$ may be a *non-degenerate* configuration (i.e., $\mathbf{x}^* \neq \mathbf{x}^0, \mathbf{x}^N$). When the dynamics parameters are such that $0 < \frac{\lambda}{\mu} < 1$ and $\gamma > 1$, the non-degenerate configurations can be explained by the presence of *denser* subgraphs, subgraphs with higher average degree than the entire network, in the underlying network $G(V, E)$.

Note that $\widehat{P}(x_i = 1)$ depends on the number of infected neighbors in the *most-probable configuration*, $\mathbf{x}^*$, not on the degree of the node in the underlying network $G(V, E)$. If a node has a small num-

ber of infected neighbors in a non-degenerate most-probable configuration $\mathbf{x}^*$, even though it may have a high degree in $G(V, E)$, then its marginal probability of infection is also small. Therefore, $\widehat{P}(x_i = 1)$ is not ranked by the degree of the ith node in $G(V, E)$. Figure 1b shows the most-probable configuration when $\frac{\lambda}{\mu} = 0.00025$ and $\gamma = 600$. We see that $m_6^* = 1$ even though node 6 has 3 neighbors in $G(V, E)$; this explains why in Figure 2b, $P(x_6 = 1)$ is smaller than the marginal probabilities of other nodes with lower degree.

4.1. Real-World Network

Real-world networks of interest are often large, precluding the computation of the marginal probabilities. Figure 4 shows the approximate marginal probabilities of a 4941-node representation of the US Western Power Grid for dynamics parameters $\frac{\lambda}{\mu} = 0.071053, \gamma = 4.0789$ [15]. This approximation is possible because the most-probable configuration can be solved efficiently when $0 < \frac{\lambda}{\mu} < 1$ and $\gamma > 1$ [9]. This approximation can also be checked against numerical approximations using sampling techniques [14]. Using $\widehat{P}(x_i = 1)$, the node with the highest degree (19 neighbors) has $\widehat{P}(x_i = 1) = 1$; however the node with the second highest degree (18 neighbors) has $\widehat{P}(x_i = 1) = 0.0663$, the minimum probability of infection of all the nodes. This means that the marginal probability of infection can not be ranked by degree.

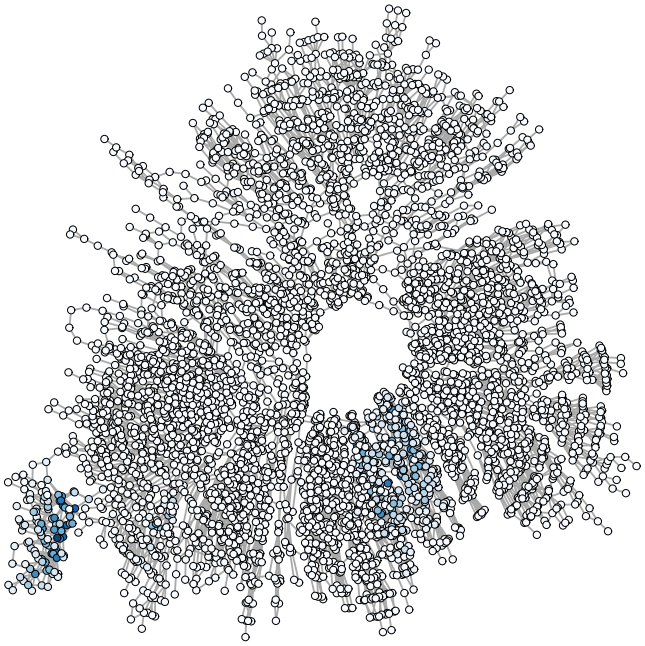

Fig. 4: $\widehat{P}(x_i = 1)$ of the US Western Power Grid for $\frac{\lambda}{\mu} = 0.071053, \gamma = 4.0789$ ($\widehat{P}(x_i = 1)$ range from 0.0663 (white) to 1 (dark blue))

5. CONCLUSION

Network-based epidemics processes assume that infection rate depends on the number of infected neighbors. Therefore, it is appealing to consider if the probability of infection of any particular node can be characterized by its connectivity in the underlying network. If this is the case, then the degree distribution can be used to rank the vulnerability of individual nodes. This paper shows that this intuition is not always true. Using a closed-form approximation of the marginal probabilities of $\pi(\mathbf{x})$, we argue that the marginal probabilities of infection $P(x_i = 1)$ may not dependent on the degree of the node in $G(V, E)$, but the degree of the node in a subgraph of $G(V, E)$ (i.e., the subgraph induced by a non-degenerate most-probable configuration).

This means that if we want the degree distribution to be an accurate reflection of nodal vulnerability then we must 1) restrict the dynamics parameters of the network process to ranges such that non-degenerate most-probable configurations do not dominate over other configurations or 2) consider only network structure $G(V, E)$ that will not result in non-degenerate most-probable configurations for any dynamics parameters (see [9]). In the future, we will consider better closed-form approximations that depend on more than just the most-probable configuration as well as relating these mathematical approximations to numerical approximations via sampling or message passing algorithms.

6. APPENDIX: PROOF FOR THEOREM 4.1

Proof. The equilibrium distribution of the scaled SIS process (3) is a Gibbs distribution. We know that the ratio of marginal probabilities is

$$\frac{P(x_i = 0)}{P(x_i = 1)} = \frac{\sum_{\mathbf{x} \in \mathcal{X}: x_i = 0} e^{H(\mathbf{x})}}{\sum_{\mathbf{x} \in \mathcal{X}: x_i = 1} e^{H(\mathbf{x})}}. \tag{8}$$

Ideally, we want to avoid summing over 2^{N-1} configurations. When $e^{H(\mathbf{x}^*)} >> e^{H(\mathbf{x})}, \forall \mathbf{x} \in \mathcal{X} \setminus \mathbf{x}^*$, we can consider only the most-probable configuration. There are 2 cases:

When $x_i^* = 0$**.** Let $T_i^+ \mathbf{x}^*$ denote the configuration that is the same as $\mathbf{x}^*$ except node i changes state to 1. Assuming $e^{H(\mathbf{x}^*)} >> e^{H(\mathbf{x})}$, we can approximate the numerator of (8) with $e^{H(\mathbf{x}^*)}$. It is a question if we can approximate the denominator of (8) with $e^{H(T_i^+ \mathbf{x}^*)}$; we argue that this is the case when the assumption regarding the dominance of the most-probable configuration is satisfied. Consider some other configuration $H(\mathbf{x}')$ where the ith node is also 0, then

$$H(T_i^+ \mathbf{x}^*) - H(T_i^+ \mathbf{x}') = H(\mathbf{x}^*) + \log\left(\frac{\lambda}{\mu}\right) + \sum_{j=1}^{N} \mathbf{A}_{ij} x_j^* \log(\gamma))$$
$$- \left(H(\mathbf{x}') + \log\left(\frac{\lambda}{\mu}\right) + \sum_{j=1}^{N} \mathbf{A}_{ij} x_j' \log(\gamma) \right)$$

Assuming that $e^{H(\mathbf{x}^*)} >> e^{H(\mathbf{x})}$, then $H(T_i^+ \mathbf{x}^*) - H(T_i^+ \mathbf{x}') > 0$ and we can (roughly) approximate (8) as

$$\frac{\widehat{P}(x_i = 0)}{\widehat{P}(x_i = 1)} = \frac{e^{H(\mathbf{x}^*)}}{e^{H(T_i^+ \mathbf{x}^*)}},$$

and show that

$$\widehat{P}(x_i = 1) = \frac{1}{1 + \left(\frac{\lambda}{\mu} \gamma^{\sum_{j=1}^{N} \mathbf{A}_{ij} x_j^*}\right)^{-1}}. \tag{9}$$

When $x_i^* = 1$**.** Let $T_i^- \mathbf{x}^*$ denote the configuration that is the same as $\mathbf{x}^*$ except node i changes state to 0, then

$$\frac{\widehat{P}(x_i = 0)}{\widehat{P}(x_i = 1)} = \frac{e^{H(T_i^- \mathbf{x}^*)}}{e^{H(\mathbf{x}^*)}},$$

resulting in the same approximation as (9).

□

7. REFERENCES

[1] J. P. Gleeson, "Binary-state dynamics on complex networks: pair approximation and beyond," *Physical Review X*, vol. 3, no. 2, p. 021004, 2013.

[2] L. Danon, A. P. Ford, T. House, C. P. Jewell, M. J. Keeling, G. O. Roberts, J. V. Ross, and M. C. Vernon, "Networks and the epidemiology of infectious disease," *Interdisciplinary Perspectives on Infectious Diseases*, 2011.

[3] T. House and M. J. Keeling, "Insights from unifying modern approximations to infections on networks," *Journal of the Royal Society Interface*, vol. 8, no. 54, pp. 67–73, 2011.

[4] M. J. Keeling and K. T. Eames, "Networks and epidemic models," *Journal of the Royal Society Interface*, vol. 2, no. 4, pp. 295–307, 2005.

[5] K. T. Eames and M. J. Keeling, "Modeling dynamic and network heterogeneities in the spread of sexually transmitted diseases," *Proceedings of the National Academy of Sciences*, vol. 99, no. 20, pp. 13 330–13 335, 2002.

[6] C. Nowzari, V. M. Preciado, and G. J. Pappas, "Analysis and control of epidemics: A survey of spreading processes on complex networks," *IEEE Control Systems*, vol. 36, no. 1, pp. 26–46, 2016.

[7] D. Chakrabarti, Y. Wang, C. Wang, J. Leskovec, and C. Faloutsos, "Epidemic thresholds in real networks," *ACM Trans. Inf. Syst. Secur.*, vol. 10, no. 4, pp. 1:1–1:26, 2008.

[8] J. Zhang and J. M. F. Moura, "Diffusion in social networks as SIS epidemics: Beyond full mixing and complete graphs," *IEEE Journal of Selected Topics in Signal Processing*, vol. 8, no. 4, pp. 537–551, Aug 2014.

[9] ——, "Role of subgraphs in epidemics over finite-size networks under the scaled SIS process," *Journal of Complex Networks*, vol. 3, no. 4, pp. 584–605, 2015. [Online]. Available: + http://dx.doi.org/10.1093/comnet/cnv006

[10] T. M. Liggett, *Stochastic Interacting Systems: Contact, Voter and Exclusion Processes*. Springer, 1999, vol. 324.

[11] P. Van Mieghem and E. Cator, "Epidemics in networks with nodal self-infection and the epidemic threshold," *Phys. Rev. E*, vol. 86, p. 016116, Jul 2012. [Online]. Available: http://link.aps.org/doi/10.1103/PhysRevE.86.016116

[12] M. Draief, A. Ganesh, and L. Massoulié, "Thresholds for virus spread on networks," in *Proceedings of the 1st International Conference on Performance Evaluation Methodolgies and Tools*, ser. valuetools '06. New York, NY, USA: ACM, 2006. [Online]. Available: http://doi.acm.org/10.1145/1190095.1190160

[13] J. Zhang and J. Moura, "Contact process with exogenous infection and the scaled SIS process," *Journal of Complex Networks*, vol. 5, no. 5, pp. 712–733, 2017. [Online]. Available: + http://dx.doi.org/10.1093/comnet/cnx003

[14] J. Zhang, "Network process: How topology impacts the dynamics of epidemics and cascading failures," Ph.D. dissertation, Carnegie Mellon University, 2015.

[15] D. J. Watts and S. H. Strogatz, "Collective dynamics of small-world networks," *Nature*, vol. 393, no. 6684, pp. 440–442, 1998.